Thin Solid Films 520 (2011) 1147–1154

Contents lists available at SciVerse ScienceDirect

Thin Solid Films

journal homepage: www.elsevier.com/locate/tsf

Effect of compressive stress inducing a band gap narrowing on the photoinduced activities of sol–gel TiO_2 films

Mohamed N. Ghazzal [a,b,*], N. Chaoui [c], M. Genet [d], Eric M. Gaigneaux [b], D. Robert [e]

[a] Laboratoire de Chimie et Methodologie pour l'Evironnement, Université Paul Verlaine de Metz, rue Victor Demange, 57500 Saint-Avold, France
[b] Institute of Condensed Matter and Nanoscience Molecules, Solids and reacTivity (IMCN/MOST), Université catholique de Louvain, Croix du Sud 2/17, B-1348 Louvain-la-Neuve, Belgium
[c] Laboratoire de Spectrométrie de Masse et de Chimie Laser, Université Paul Verlaine de Metz, Boulvard arago, F-57078 Metz Cedex 3, France
[d] Institute of Condensed Matter and Nanoscience Molecules, Division of "Bio and Soft Matter (IMCN/BSMA), Université catholique de Louvain, Croix du Sud 2/17, B-1348 Louvain-la-Neuve, Belgium
[e] Laboratoire des Matériaux, Surface et Procédés pour la Catalyse (LMSPC) CNRS-UMR7515, Antenne de Saint-Avold, UPV-Metz, Rue Victor Demange 57500 Saint-Avold, France

ARTICLE INFO

Article history:
Received 28 April 2011
Received in revised form 26 August 2011
Accepted 26 August 2011
Available online 2 September 2011

Keywords:
Titanium oxide
Thin film
Photocatalysis
Photoinduced hydrophilicity
Compressive stress
Band gap

ABSTRACT

TiO_2 thin films grown on different kinds of substrates were obtained by sol–gel process. X-ray diffraction revealed that the TiO_2 lattice parameter *c* decreased continuously, indicating a continuous variation in the compressive stress, a negligible compressive stress of the film grown onto Soda-Lime Glass (SLG), medium compressive stress of the film grown onto BoroSilicate Glass (BSG) and large compressive stress of the film deposited onto the Quartz Substrate (QS). UV–Vis absorbance spectra exhibited a red-shift of the absorbance edge of the TiO_2 films suggesting a lowering of the band gap, which is a direct consequence of the increase of the compressive stress. X-ray photoelectron spectroscopy revealed that the surface composition of titania films was similar except for sodium-ion concentration. The rate observed during the photo-oxydation of the stearic acid on TiO_2/QS was twice as high as that of TiO_2/BSG and about 1000 times superior to that of TiO_2/SLG. The photoinduced wettability shows an identical dependence of the compressive stress. According to these results, the compressive stress could be used to tune the band gap of the titanium oxide in order to enhance the photoinduced properties.

1. Introduction

Photoactive TiO_2 semiconductor using low-energy UV has lead to widespread scientific and technological interest. Besides the photo-oxidative activity of TiO_2 surfaces, UV-induced hydrophilicity effects on TiO_2 present a second extraordinary characteristic. Taking advantage of the combination of these two phenomena self-cleaning surfaces constitute an area where the transition from a promising technology to global market product ranges has occurred. Since the pioneering work of Fujishima and Honda [1], the photocatalytic mechanism of the TiO_2 surface was largely studied [2–4]. The prevalent mechanism is based on photogenerated electron-holes pairs that are able to migrate to the surface and eventually interact with oxygen and adsorbed hydroxyls groups thus participating in the photocatalytic reaction. In contrast, the mechanism for photoinduced hydrophilicity still remains unclear. Most of the proposed models for this effect involve a structural change of the photocatalyst surface. On the other hand, the dissociative adsorption of H_2O molecules on the oxygen vacancies leads to an increase in the number of the surface hydroxyl groups of the semiconductor during UV light irradiation [5,6]. It has been found that in the dark the hydroxyl groups newly formed on the TiO_2 surface after UV irradiation can be oxidized by O_2 and that the oxygen vacancies can be recovered thus gradually turning the surface hydrophobic [5,7]. White et al. [8] have revealed by temperature programmed desorption measurement of TiO_2 (110) single crystal that neither H_2O dissociation nor oxygen vacancies are related to the hydrophilic conversion. Takeushi et al. [9] proposed that the photoinduced hydrophilic conversion of TiO_2 surface originated from the desorption of H_2O molecules from the photocatalyst surface caused by a heating of the surface during irradiation, and by the photocatalytic decomposition of adsorbed hydrocarbons. Others works reported that the hydrophilicity was simply a consequence of the cleanup of the surface through a photocatalytic oxidation of hydrophobic thin contamination layers [10–12].

Many efforts have been made to improve the photoinduced activity of titanium films. In the case of photocatalytic activity, reducing the number of photogenerated electron-hole pairs has been extensively explored. To do so, one possibility consists on coupling a large band gap semiconductor with a smaller band gap semiconductor, the latter presenting suitable potential energies [13,14]. The process not only helps for charge separation by isolating electrons and holes into two distinct particles but, at the same time, it allows the extension of the photoresponse of the photocatalyst in the visible range.

* Corresponding author at: Institute of Condensed Matter and Nanoscience Molecules, Solids and reacTivity (IMCN/MOST), Université catholique de Louvain, Croix du Sud 2/17, B-1348 Louvain-la-Neuve, Belgium. Tel.: +32 10 47 36 60; fax: +32 10 47 36 49.
E-mail address: mohamed.ghazzal@uclouvain.be (M.N. Ghazzal).

0040-6090/$ – see front matter © 2011 Elsevier B.V. All rights reserved.
doi:10.1016/j.tsf.2011.08.097

On the other hand, several studies reported that it is possible to improve the photocatalytic activity of TiO_2 by doping with foreign elements [15–17]. Doping of TiO_2 affects its bulk electronic structure, namely, the position of the Fermi energy level, the formation of new energy levels by the interaction of an interstitial dopant with the semiconductor lattice, the electron conductivity in the bulk semiconductor, the surface properties of the thickness of the space charge layer. However, some dopants, such as metallic cations, have the disadvantage that they can give rise to localized d-levels deep in the band gap of TiO_2 which often serve as recombination centers for photogenerated charge carriers. Thus, anionic non-metal dopants, especially nitrogen, appear to be more appropriate for extending the photocatalytic activity of TiO_2 to the visible light region since their p states contribute to the narrowing of the band gap by mixing with O 2p states [18]. In fact, the efficiency of the hydrophilic conversion of the titanium surface was improved by increasing the hydroxyl groups at the surface. Guan et al. [19] reported that when mixing SiO_2 and TiO_2 they form single oxide particles in the films, but with a part of complex oxide may be formed. They suggest that Ti – O – Si bonds increase the surface acidity which induces an increase of hydroxyl content in the composite films. Recently, Houmard et al. [20] reported that TiO_2–SiO_2 composite films increase the ratio of adsorbed hydroxyl groups at the surface thus leading to coatings with a natural super-hydrophilicity persistence and easy photoregeneration.

Titanium film grown onto a substrate often requires heat treatment followed by cooling step in order to obtain the photoactive phase; c.a. anatase. During these steps, the structural properties can be strongly influenced. The films were, often, subject to a residual constrain induced by the discrepancy of the thermal expansion coefficient between the film and substrate. Shibata et al. [21,22] controlled the residual stress in titania films, deposited *via* the RF reactive magnetron sputtering method onto different kinds of substrates, to induce a surface structural change and then to enhance the rate of the hydrophilic conversion. Aubry et al. [23] reported that the titanium film grown by RF reactive magnetron sputtering onto glass substrate and calcined at increasing temperatures shows a photoinduced activity optimum at 400 °C. They supposed that, at other temperatures, structural defects induced by internal (tensile or compressive) stress could create energy levels in the band gap of the TiO_2 semiconductor, favoring the charge carrier capture and thus their recombination. Other studies also have shown that strain can be used to enhance the TiO_2 photoelectrochemical efficiency [24,25]. However, little attention has been paid to the influence of the residual stress in the structural properties of TiO_2 films and its relationship with photoactivity.

In this paper, we investigate the effect of the residual stress in the photoinduced properties of the TiO_2 film. We show that residual stress induces a physical modification on the TiO_2 structure and improves its photoinduced abilities. The titania films were prepared via a sol–gel method and grown onto different kinds of substrates in order to introduce variable residual stress. The photoactive properties of each film were evaluated. The effects of the residual stress on the structural and optical properties of titanium film were also investigated.

2. Experimental section

The procedure used for the preparation of the titania films is described in detail elsewhere [26]. Briefly, titanium(IV) isopropoxide was used as a precursor to synthesize the titania sol via an acid catalyzed sol–gel process at room temperature in the following way: 10 ml of $Ti(OC_3H_7)_4$ was dissolved in 50 ml of absolute ethanol under magnetic stirring and 1,3 ml of HCl was added to catalyze the hydrolysis. After stirring during 30 min, the obtained solution was hydrolyzed by the addition of a mixture of water (0,6 ml) and absolute ethanol (50 ml) drop-wise keeping stirring for another 2 h. The synthesis was carried out under argon atmosphere. The resultant TiO_2 sol was clear and stable for some weeks. The pH of the prepared TiO_2 sol was close to 1.

To prepare the TiO_2 thin films aiming to obtain different photocatalytic activity, the films were grown onto three kinds of glass substrates (75 mm × 25 mm × 1 mm) of variable thermal expansion coefficient (see Table 1). The following substrates were used: Soda-Lime Glass (SLG), BoroSilicate Glass (BSG) and Quartz Substrate (QS). The substrates were dipped into and pulled out from the solution at a velocity of 11,5 cm.min^{-1} and then they were dried in air at 70 °C for 5 min. The dip-coating process was repeated 36 times at ambient atmosphere. The as-prepared films were dried overnight at 80 °C and then heated in air for 2 h at 450 °C using a heating rate of 5 °C.min^{-1}. The substrates were cleaned with detergent and with ethanol under ultrasonication for half an hour, and then rinsed with distilled water and dried for 1 h at 100 °C prior to use. The contact angle measured for all substrates after the cleaning procedure was inferior to 10°. At these conditions a perfect wetting of the sol is allowed whatever the substrate nature, and it is possible to improve the affinity between the surface of the glasses and the TiO_2 sol-precursor during the coating process.

The coating morphology was investigated by scanning electron microscopy (SEM) using a Philips XL30 SFEG equipped with a field effect gun operating at 5 kV. The structural properties were investigated by X-ray diffraction (XRD) by means a diffractometer Siemens D500 in Bragg–Brentano configuration using a Co-Kα (λ = 0,17889 nm) radiation at a grazing incidence of 0,05°. Silicon powder was dispersed on the coating surface in order to calibrate the diffractograms according to the procedure described by Aubry et al. [23].

Diffuse reflectance spectra of titania films were recorded by means of a UV–Vis spectrophotometer (Perkin-Elmer) equipped with an integrating sphere. The baseline was calibrated by $BaSO_4$ in the diffuse reflectance mode. The spectra were recorded at room temperature in the spectral range 200–800 nm.

X-ray photoelectron spectroscopy (XPS) was performed on a Kratos Axis Ultra spectrometer (Kratos Analytical, Manchester, U.K.). The samples were fixed on the support using a double-sided adhesive conducting tape. The residual pressure in the analysis chamber was lower than 10^{-6} Pa. The monochromatic Al X-ray source was powered at 15 kV and the emission current was 10 mA. The charge stabilization was achieved by using the Kratos Axis device. Analyses were performed in the hybrid lens mode with the slot aperture and the iris drive position set at 0,5 inch; the resulting analyzed area was

Table 1
Comparison of d-spacing, cell parameters, thermal expansion coefficients and residual stress for each sample.

Substrate	α_s x 10^{-6}/°C	σ_{th}^{*}(MPa)	$d(101)$	$\sigma_{d(101)}$ (MPa)	$d(004)$	$\sigma_{d(004)}$ (MPa)	a (nm)	c (nm)
SLG	8,6	0	0,3512	1127	0,2365	2712	0,37823	0,946
BSG	3	614	0,3509	1550	0,2346	6676	0,37835	0,9384
QS	0,5	888,16	0,3492	3946	0,234	7928	0,37637	0,936

* σ_{th} was a thermal stress caused by a bimetal effect between the film and the substrate, which was determined by the following equation $\sigma_{th} = E_f(\alpha_f - \alpha_s) \times \Delta T$. Where E_f is Young's modulus for the film, and α_f and α_s are thermal expansion coefficients of the film and the substrate, respectively.

700 μm × 300 μm^2. A pass energy of the analyzer was set at 160 eV for the survey scan and 40 eV for the narrow scans. The binding energy (BE) values were referred to the C-(C, H) contribution of the C1s peak fixed at 284,8 eV. The data treatment was performed with the Casa XPS software (Casa Software Ltd., UK). The peaks were decomposed using a linear baseline, and a component shape defined by the product of a Gauss and Lorentz function, in the 70:30 ratio, respectively. Molar concentration ratios were calculated using peak areas normalized according to the acquisition parameters and the relative sensitivity factors and transmission function provided by the manufacturer.

The photocatalytic degradation of the organic hydrocarbon model and the kinetics of the hydrophilic conversion of the TiO_2 surfaces were measured separately as a function of irradiation time. A Solar box ATLAS Suntest CPS + apparatus provided with a Xenon lamp simulating natural radiation was used for all experiments. The apparatus was also equipped with an IR cut-filter and air cooling system. The temperature inside the box did not exceed 25 °C as measured by a thermocouple. The power density in the UVA and the UVB range was 0,25 mW.cm^{-2} and 0,016 mW.cm^{-2} as measured by a powermeter (Delta Ohm 2101).

The photocatalytic performances were estimated by following the degradation rate of a Stearic Acid (SA hereafter) for each system (TiO_2/SLG, TiO_2/BSG and TiO_2/QS). The photocatalyst surfaces were recovered by a SA by dip coating the samples in a methanolic solution of SA (0,02 mol.l^{-1}) and then drying in air. The disappearance of SA from the surface was achieved by measuring the integrated absorbance over the 2700–3000 cm^{-1} infrared range. The necessary infrared measurements were made with a Fourier transform infrared (FTIR) spectrometer (BIO-RAD, FTS 165).

The contact angle of sessile water drops on test substrates (TiO_2/Substrate) was measured using a homemade apparatus. The system comprises a SONY AVC-D5/D7CE camera interface via an adaptor with a computer loaded with an appropriate PEGASE software. The software package associated with the instrument allowed calculation of the contact angle made by the water droplet deposited on the substrate through curve-fitting of the droplet image outline. The experiments were carried out under ambient conditions with temperature ranging between 21 and 24,5 °C and relative humidity ranging between 46 and 54 %. The droplet size used for the measurements was 3 μl.

3. Results and discussions

3.1. Structure and surface morphology

In Fig. 1a–1c typical SEM images of surface-films annealed at 450 °C are shown. The surface images of the film dip-coated on SLG revealed the presence of cracks whose orientation seems to be similar all over the film. These cracks can be explained by considering the large difference in the thermal expansion coefficient between the substrate and the titania films as it has been frequently reported and suggested by several authors. In one hand, it has been recognized that residual compressive stresses may cause a film delamination from the substrate whereas tensile stress may cause surface cracks in the film [27,28]. In other hand, related the method employed in our experiment, dehydration or solvent trap can occurs. During the calcinations step, dehydration removes surface-bound Ti-OH groups and increases shrinkage into the film (formation of Ti–O–Ti). In general, the average thickness of the film was reduced after annealing. This shrinkage in thickness signifies the dehydration of water from the TiO_2 film and could induce a crack formation [29]. Also the solvent can be trapped within the close porosity of the film during the condensation. The heat treatment increases the pressure under the pore and an internal stress is created leading to the distortion of the film and liberation of the solvent leading to a cracks formation. However, in our case there was no difference between the expansion coefficient

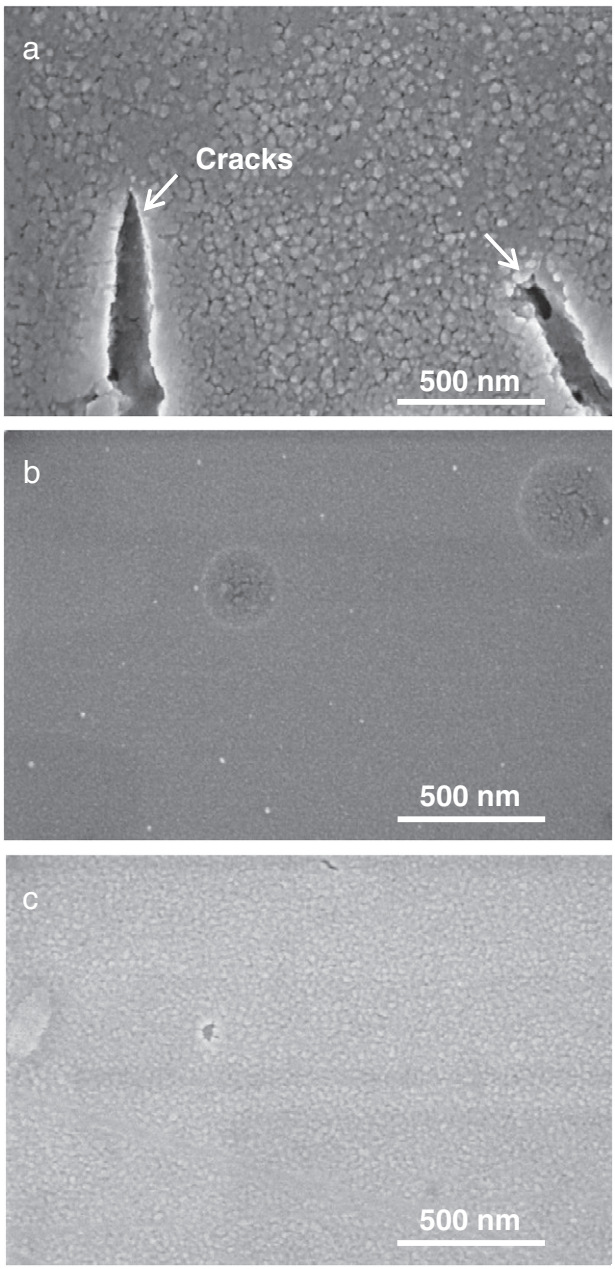

Fig. 1. SEM images of the TiO_2 films surface (a) TiO_2/SLG, (b) TiO_2/BSG and (c) TiO_2/QS after calcination at 450 °C.

of the film and the SLG substrate ($\alpha_{SLG} = \alpha_{TiO_2} = 8{,}6 \times 10^{-6}$/C°) and no difference was observed between the morphology of TiO_2/QS and that of TiO_2/BSG. The films grown on the FS and BSG presented no evidence of surface cracking, and they were neither affected by the solvent evaporation nor by the dehydration upon heating (even using the same procedure). This suggests that the origin of the cracks probably results from the internal strain induced by the diffusion of Na^+ ions throughout grain boundaries. It is well known that during the calcination step of TiO_2 films grown on SLG (containing approximately 14 % of sodium among other alkali elements of NaO), alkali ions, particularly Na^+, are likely to diffuse from the substrate to the coating [30–32]. The films presented a granular structure with grains sizes of ≈30–50 nm for TiO_2/SLG and finer ≈10–30 nm for TiO_2/FS and TiO_2/BSG.

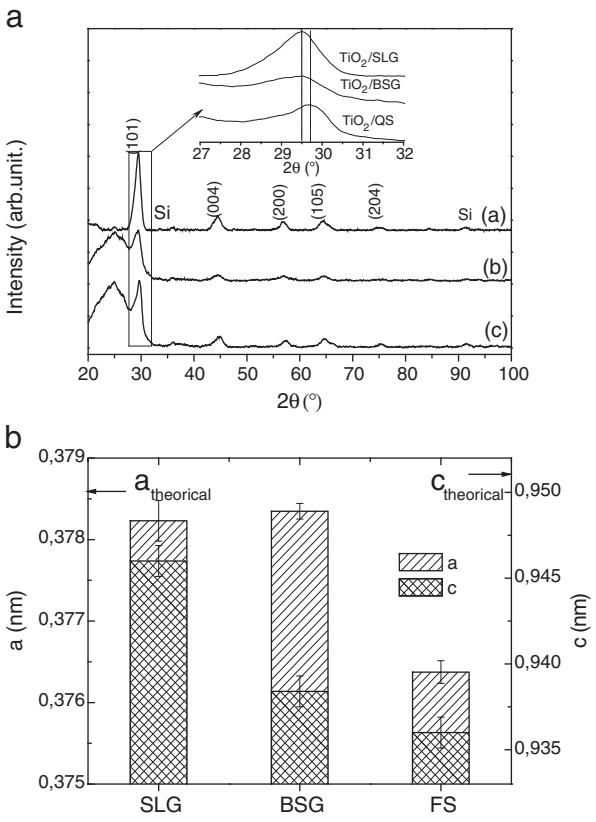

Fig. 2. (a) Grazing incidence X-ray diffraction pattern of the TiO_2 films deposited on the different glasses (a) SLG, (b) BSG and (c) QS. (b) Evolution of the anatase cell parameters with the nature of the substrate.

X-ray diffraction (XRD) measurements were used to investigate the crystal structure of the sol–gel films. XRD patterns confirmed that the films are crystalline and a predominance of the anatase structure with a preferential (101) orientation (Fig. 2a). The peak position of the (101) direction was slightly shifted compared to the initial position (JCPDS File No. 21–1272). The observed shift proves that the post-treatment, needed to obtain the anatase phase, induces a residual stress due to the difference in the thermal expansion coefficient, especially in the case of TiO_2/BSG and TiO_2/QS. The TiO_2 deposited on SLG shows a weak residual stress since d-spacing along the (101) direction (see Table 1) was slightly inferior from the theorical value ($d_{(101)}$ = 0,352 nm, JCPDS File No. 21–1272). However, the shift was more noticeable for QS.

The textural change in the titania films grown on variables substrates allows determining the cell parameters using the following formulae for tetragonal symmetry:

$$c = 4\times d_{004} \tag{1}$$

$$a = \frac{d_{101}\times 4d_{004}}{\sqrt{16d_{004}^2 - d_{101}^2}}. \tag{2}$$

Fig. 2b shows the cell parameters of the TiO_2 coating for different systems. In comparison with the theoretical value, all cell parameters were lower (a = 0,3785 nm and c = 0,9514 nm from the JCPDS 00-021-1272 card number), indicating that the coatings are submitted to compressive stress. The low temperature sol–gel processed films possess a shorter out-of plane lattice parameter due to an in-plane residual stress [33] hence corroborating our results.

In order to understand the strain effect on both *a* and *c* cell parameters, the residual stress was calculated from the lattice spacing of the anatase films for the (101) and the (004) direction. The dependence of the lattice strain ε of the anatase on the direction and on the residual stress σ of the films were defined as follows [21]:

$$\varepsilon = \frac{d^{\circ}_{hkl} - d_{hkl}}{d^{\circ}_{hkl}} \tag{3}$$

$$\sigma = \frac{E\varepsilon}{2\nu}. \tag{4}$$

Where, $d^{\circ}_{(hkl)}$ and $d_{(hkl)}$ are the lattice spacing in the film and in the bulk in respect to the (hkl) plane. *E* is Young's modulus, and ν is Poisson's ratio of the film. To roughly estimate the residual stresses of the films, Poisson's ratio and Young's modulus for the anatase phase were assumed to be 0,26 and 258 GPa [21], respectively. The calculated thermal stresses and observed residual stresses are summarized in Table 1. A relatively good correlation was observed between the evolution of the cell parameters and the corresponding residual stress. The *a* cell parameters remained constant along the (101) direction for SLG and BSG, whereas it was twice higher for QS. In turn, the greater the compressive stress in the film along the (004) direction was the lower the *c* cell parameter was. The decrease in the *c* lattice parameter under compressive stress suggests a shortening of the lattice distance between the Ti–Ti atoms along the (004) direction. The evolution of the cell parameters varied independently from the thermal stress, therefore corroborating the evolution of the residual strain. These results show that the difference in the thermal expansion coefficient is most likely not responsible for the significant modification of nanocrystalline anatase structure observed in the sol–gel annealed films. The residual stress in the titania films was the main dominant effect, particularly along the (004) direction. These results diverge from those reported by Shibata et al. [21]. These authors demonstrated that the thermal stress can be used to control the residual stress of titania films grown on different kinds of substrates thence to the evolution of the d-spacing. The difference can be explained by considering the procedure adopted for the elaboration of the materials. Contrary to Shibata et al. who use a physical deposition to obtain the anatase films, the pyrolysis and densification in the sol–gel process derived film lead to the evolution of in-plane residual stress [33]. Furthermore, the reduction of the out-of-plane lattice parameter suggests that the densification was more vigorous [34,35] and leads to the increase of the residual stress for SLG, BSG and QS respectively.

Fig. 3a shows the UV–Vis absorption spectra of TiO_2 films grown onto different substrates. The absorption edge of TiO_2/SLG was observed at about 340 nm whereas that of TiO_2 films grown onto BSG and QS were at about 360 and 375 nm, respectively. Therefore a red-shift of the adsorption edge of the titanium film was clearly identified. That the compressive stress extended the absorbance specter of the TiO_2 films to higher wavelengths suggests that a lowering of the band gap of the semiconductor has occurred. In this sense, the present results were in accordance with other studies [25,36,37] reporting that the band gap of a conventional semiconductor is usually sensitive to external pressure or volume deformation. The band gap was determined by plotting $(\alpha h\nu)^2$ versus $(h\nu)$ [38]. We have assumed that the sensitivity αd (α: being the absorption coefficient and d being the film thickness) should be of the order of unity or $d \approx 1/\alpha$ and that the scattering was negligible. Fig. 3b shows band gap narrowing from 3,68 eV for TiO_2/SLG with negligible compressive stress, 3,49 eV for TiO_2/BSG for medium compressive stress to 3,35 eV for TiO_2/QS for large compressive stress.

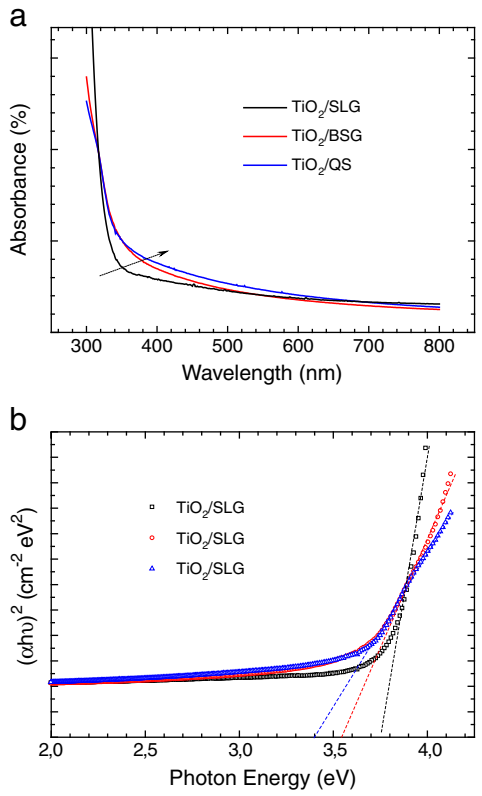

Fig. 3. (a) UV–Vis absorption results of films grown on different substrate, (b) variation of $(\alpha h\upsilon)^2$ versus hυ of the titania thin films.

Ellipsometry measurements (not included) revealed that the films have thickness values of 41 nm and 42 nm for TiO_2/BSG and TiO_2/QS, respectively [26]. An optical index of 2,17 at 630 nm was found for both samples. This value is in good agreement with the values reported in other works for sol–gel anatase thin films [39]. The TiO_2/SLG film thickness was estimated from the cracks observed on the SEM images. This feature allowed to roughly estimate the film thickness at 50–60 nm.

Table 2
Surface composition content of titania films as determined by XPS expressed by at %.

Samples	O–Ti	Ti 2p	O=C.O-C.-OH	C-(C.H)	Cl 2p	Si 2p	Mg 2p	Na 1 s
TiO_2/SLG	37,3	19,3	12,4	13	0,8	1,3	4,8	7,7
TiO_2/BSG	32,4	18,7	12,8	25	–	0,7	5,8	<1
TiO_2/QS	21,8	13,1	15,7	32	0,1	0,9	4,3	<1

An example of a general XPS spectrum of a TiO_2/SLG thin film is shown in Fig. 4a. Whatever the system, the characteristic peaks of titanium, oxygen and carbon can be observed. Furthermore, other species such as Si 2p, Mg 2p, Cl 2p (Ca 2p, K 2p as traces <0,1 %) and Na 1 s were detected. It is well known that during the annealing step alkali elements, such as Na, diffuse from the substrate to reach the coating [31]. The concentration of each element is summarized in Table 2 for all samples. XPS analysis indicates an O/Ti atomic ratio between 1,6 and 1,9, with a carbon content ranging from ~12 to 30 %. In Fig. 4b, the high – resolution XPS spectrum of Ti 2p shows intense peaks for Ti 2p3/2 and Ti 2p1/2 centered at the binding energy values of 458,48 eV and 463,16 eV, respectively. The measured separation between the Ti 2p3/2 and Ti 2p1/2 peaks was 5,7 eV and it corresponded to the binding energy separation observed for stoichiometric TiO_2 [40]. The rather TiO_2 crystalline structure was confirmed by XRD. The C 1 s was deconvoluted into three peaks (Fig. 4c). The peak centered at 284,8 eV was attributed to the hydrocarbon adsorbed at the surface and the peaks at 286,3 and 288,5 eV were ascribed to carbon linked to oxygen in different forms. The asymmetric O 1 s region was deconvoluted into two

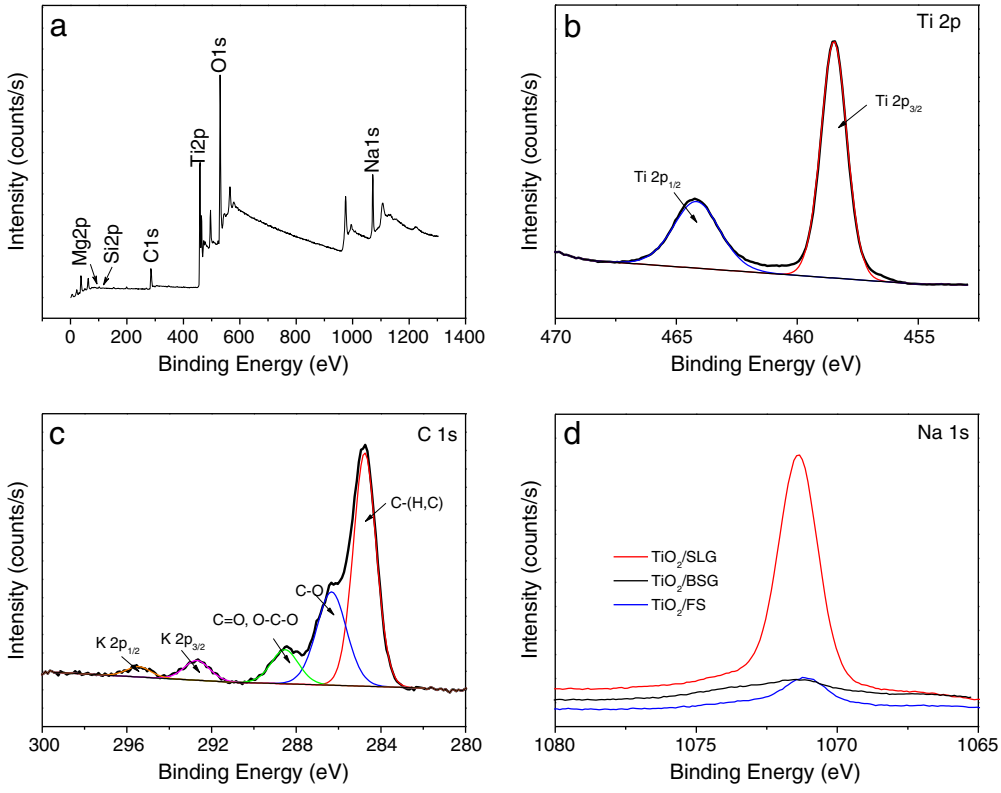

Fig. 4. XPS spectra of the surface of TiO_2 film.

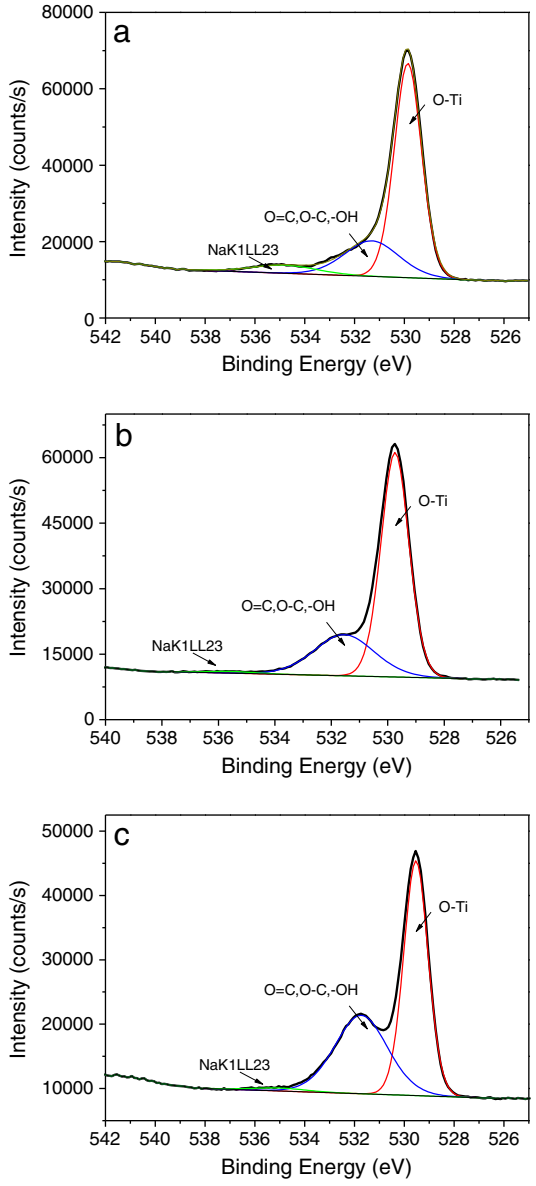

Fig. 5. XPS peaks of the O 1 s region for each titanium film (a) TiO_2/SLG, (b) TiO_2/BSG and (c) TiO_2/QS.

peaks (Fig. 5a–5c). The main peak centered at the binding energy of 529,8 eV was attributed to the Ti – O bonds of TiO_2. The shoulder on the left-hand side of the O 1 s peak and centered at 531,4 eV was assigned to oxygen linked to carbon and to the O – H bonds of the hydroxyl groups of TiO_2. XPS analysis at O 1 s region, before UV-irradiation, did not reveal any structural change. The result suggests that the compressive stress has no influence on the hydroxyl species adsorbed at the surface. The sodium content was found to vary from less than 1 % to 7,8 % depending on the substrate (Fig. 4d). Indeed, the Na^+ content was less than 1 % for BSG and QS, and was higher for SLG based substrates. This result was in accordance with earlier studies discussing the diffusion of sodium-ions from the substrate to the titania films during the annealing step [31,41,42]. However, it was difficult to quantify the sodium-ion content at the surface of the films grown on BSG and QS, because of the low sodium-ion content at the titania surface and also to the superposition of the Na 1 s peak with that of the $TiKL_1L_1$ Auger peak.

3.2. Titania films photoactivity

The photocatalytic activity of the films was quantitatively evaluated by comparing the degradation rate of SA. The overall process can be summarized by the following reaction equation [30,43]:

$$CH_3(CH_2)_{16}CO_2H + 26O_2 \xrightarrow{h\nu \geq E_{BG}+TiO_2} 18CO_2 + 18H_2O. \quad (5)$$

It was assumed that the *global* reaction rate of the degradation of the SA monitored by FTIR can be described by the kinetic model corresponding to a pseudo–first order reaction as suggested by Suwunyama et al. [44]. The photocalytic activity was expressed in terms of apparent kinetic constant K_{app}. This constant was obtained by plotting $\ln([SA]_0/[SA])$, where [SA] is the concentration at a given time as a function of time on stream. Fig. 6a illustrates a typical FTIR adsorption spectra collected periodically *versus* illumination time for TiO_2/QS system. From the data in Fig. 6a, it is clear that as illumination time increased the SA molecules disappear, with peaks in the range 2700–3000 cm^{-1}. Fig. 6b shows a comparison of the apparent constant rate for the degradation of SA using the various titania films. The degradation rate observed for TiO_2/QS was 1000 times higher than that registered for TiO_2/SLG and about 50 % higher than that for TiO_2/BSG.

The changes of the contact angle under UV irradiation can be followed from the results presented in Fig. 7a. The initial values of the contact angle were 37,6 ± 0,8°, 31,6 ± 0,9°, and 37,4 ± 0,8° for TiO_2/SLG, TiO_2/BSG and TiO_2/QS, respectively. The difference in the initial values of the contact angle between the TiO_2/BSG and TiO_2/QS is considered to be caused by a difference in the concentration of surface carbon contamination of the films, as revealed by XPS analysis. However, the high contact angle value observed for TiO_2/SLG should be

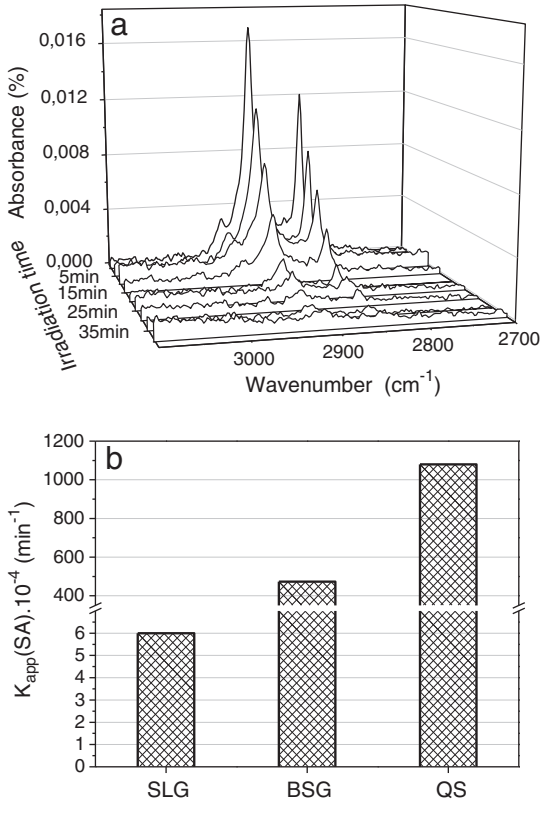

Fig. 6. (a) FTIR absorbance versus wavenumber spectra recorded for a sample of TiO_2/FS coated with stearic acid, as a function of irradiation time and (b) disappearance rate (apparent kinetic constant K_{app}) of the SA coated TiO_2/SLG, TiO_2/BSG and TiO_2/QS.

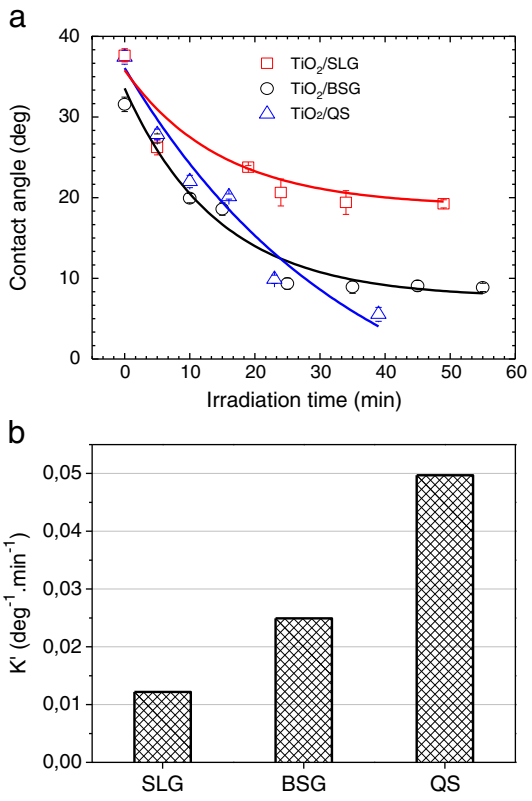

Fig. 7. (a) Changes in water contact angles of titania thin films grown on different kind of substrate, (b) the rate constant of the hydrophilic conversion of TiO_2/SLG, TiO_2/BSG and TiO_2/QS.

due to the surface roughness. The contact angle decreased with UV irradiation time for all samples. A similarity between the photoinduced hydrophilic conversion efficiency and the photocatalytic activity of the titania films was observed. Whereas the hydrophilic conversion of the photocatalyst surface grown on SLG was the slowest, those grown on BSG and QS showed a faster rate conversion versus the irradiation time. The kinetic constant of the hydrophilic conversion is showed in Fig. 7b, according to the work previously reported by Sakai et al. [45]. Indeed, the hierarchical order established for the kinetic degradation of SA was well correlated to the hydrophilic conversion of the titania surfaces. These results clearly suggest the existence of a dependency of the photoactive properties of the TiO_2 films on the substrate compressive stress.

Let us discuss the dependence of the photoactive properties on the substrate. The main difference observed between the films properties could be the compressive stress. Indeed, the rate of photocatalytic activity and the hydrophilic conversion exhibits higher performance when the residual stress increases in the film (see Table 2). However, in the case of the TiO_2/SLG, neither the small residual stress, nor the smallest absorption edge allows explaining the weak photoactive performance. Indeed, it was reported that the photocatalytic activity of sol–gel titania films grown on sodium—ion rich substrates was sensitive to the diffusion of the Na^+ ion [30–32,42] to the surface. Nam et al. [31] revealed that Na^+ ions diffused from the SLG substrate, raised the temperature required for anatase formation and gave rise the particle size of the TiO_2 thin films, hence resulting in a reduction of the photocatalytic activity. Watanabe et al. [42] reported that the sodium—ion acts as a recombination center of the photogenerated e^-/h^+ pairs in order to explain the deterioration of the photocatalytic activity of the titania films. In the same study, they showed that the photoinduced hydrophilic conversion is not influenced by the diffusion of the sodium-ion. In contrast, we observed a dependence of the sodium—ion concentration on both the photocatalytic activity and the photoinduced hydrophilic conversion. The TiO_2/SLG sodium—ion rich film (7,8 %, XPS data) had a grain in size greater than that of the TiO_2/BSG and of the TiO_2/QS sodium—ion poor film (<1%, XPS data). This result suggests that the diffusion of the sodium—ion through the grain boundary rises the crystallization temperature hence the size of the grains. The latter leads to a modification of the surface area of the films (at the molecular level) and causes a deterioration of their photoactive properties.

Actually, titania films grown on BSG and QS exhibited comparable grain size, thickness, surface area and chemical surface composition. Nevertheless, they showed variable photoactive properties and variable residual stress; particularly, a medium compressive stress for TiO_2/BSG and a large compressive stress for TiO_2/QS. The results show that as the compressive stress increases, the photoactive performance was significantly improved. Contrary to the findings presented herein, Shibata et al. [21] reported that the photocatalytic oxidative decomposition of cis-9-octadecenoic acid shows no stress dependence while the photoinduced hydrophilic conversion shows a remarkable stress dependence [21,22]. The authors explained their results by considering that a separate and an independent mechanism occurred during the photocatalytic degradation and the photoinduced hydrophilicity.

In our case, the distortion of the *c* lattice parameter under compressive stress rather suggests a reduction of the lattice distance of Ti–Ti atoms. This compressive stress reduces the TiO_2 band gap and extends the photoresponse of the photocatalyst at a higher wavelength (Fig. 3). The energy of the excitation of the TiO_2 photocatalyst becomes lower for TiO_2/QS than that for TiO_2/BSG and TiO_2/SLG. To explain the enhancement of the rate of photocatalytic degradation of SA, both the band gap reduction and the weal carrier loss can be considered. The compressive stress reduces the band gap energy and extends the absorption edge of TiO_2 to a higher wavelength, which in turn allows the photocatalyst absorbing more energy from the UV range. Since the degradation of SA could result of a direct reaction with photogenerated electrons/holes and/or photooxidation via the formation of highly reactive oxidant species. These latter are products of the reaction involving the adsorption of species (H_2O and O_2) on the TiO_2 surface. In the basis of the photocatalytic mechanism, the number of the holes photogenerated at the TiO_2/QS surface can be estimated to be approximately half of that on the TiO_2/BSG surface, since the surface properties were nearly identical, and the degradation rate of SA was nearly half of that of TiO_2/BSG. This result seems reasonable, since TiO_2/QS photocatalyst with large compressive stress might have more photogenerated carriers as compared to the TiO_2/BSG photocatalyst possessing medium compressive stress due to the decrease in the surface defect. Based on both observation and the work of Yin et al. [24], we suggest that the compressive stress keeps the material defect-free, thus, improve its carrier collection. The photogenerated holes react with the adsorbed water producing more $OH^{\bullet}$ radicals that oxidize SA. These features can help rationalizing the reasons behind the improvement of the photocatalytic activity with the compressive stress but not with the rate of the hydrophilic conversion. In one hand, the power density reached for the photocatalyst surface was about $(0{,}25 + 0{,}016)$ mW.cm^{-2}. This value was four time lower than that used by Takeushi et al. [9] (1 mW.cm^{-2}). Since the model proposed by Takeushi was based on the desorption of H_2O molecules from the TiO_2 surface during UV irradiation by heating effect of the light source, the decrease of the amount of H_2O molecules leads to reduction of the distribution of the hydrogen bonds resulting in the formation of H_2O thin layer. The low flux used in our study avoid heating of the photocatalyst surface and allowed to exclude partially that model to explain the photoinduced wettability since any variation of the temperature at the photocatalyst surface (measured by a thermocouple) was observed during UV-irradiation. In other hand, the combination of the two mechanisms describing the hydrophilic conversion should be involved somehow. The photocatalytic oxidation of the hydrocarbon monolayer at the surface of the films is responsible for the reduction of

the contact angle at the high range (from ~30° to ~10°) [8,10,11], and the evolution of the compressive stress contributes actively to that process. However, below the value of 10° the mechanism for inducing the change in contact angle becomes complex. The UV illumination probably induces a structural change on the photocatalyst surface and an adsorption of metastable OH groups occurs. This mechanism was contemplated in order to explain this phenomenon. This concept was reviewed by Fujishima et al. [46]. On the basis of Fujishima's concept, we can assume that the compressive stress improves the carrier collection that reacts with the adsorbed water and leads to bond breakage, which might be improved by the hydroxyl group of the titanium surface.

4. Conclusion

Titania films with variable compressive stress on different substrates were obtained *via* dip-coating of a precursor sol. After treatment at 450 °C, a distortion of the lattice parameters was confirmed by XRD patterns at different levels. The sol–gel titania films were very sensitive to the stress induced by the thermal expansion. The pyrolysis and densification in the sol–gel process led to the evolution of in-plane residual stress. The decrease of the out-of-plane parameter suggests that the densification was more vigorous. The compressive stress reduces the lattice space between neighboring Ti atoms. We showed that the compressive stress can be considered in order to improve the TiO_2 photoinduced activities. The photoinduced performance was improved by extending the absorption spectrum of the titanium film at a higher wavelength and by increasing the photogenerated carrier collection.

Acknowledgment

The authors thank E. Aubry for XRD and SEM measurements. M.N.G. is grateful to Ghislaine Gris for valuable comments on the manuscript.

References

[1] A. Fujishima, K. Honda, Nature 238 (1972) 37.
[2] M.A. Fox, M.T. Dulay, Chem. Rev. 93 (1993) 341.
[3] A.L. Linsebigler, G. Lu, J.T. Yates Jr., Chem. Rev. 95 (1995) 735.
[4] A. Mills, S. Le Hunte, J. Photochem, Photobiol. A 108 (1997) 1.
[5] R. Wang, K. Hashimoto, A. Fujishima, M. Chikuni, E. Kojima, A. Kitamura, M. Shimohigoshi, T. Watanabe, Adv. Mater. 10 (1998) 135.
[6] R. Wang, K. Hashimoto, A. Fujishima, M. Chikuni, E. Kojima, A. Kitamura, M. Shimohigoshi, T. Watanabe, Nature 388 (1997) 431.
[7] N. Sakai, R. Wang, A. Fujishima, T. Watanabe, K. Hashimoto, Langmuir 14 (1998) 5918.
[8] J.M. White, J. Szanyi, M.A. Henderson, J. Phys. Chem. B 107 (2003) 9029.
[9] M. Takeushi, K. Sakamoto, G. Martra, S. Coluccia, M. Anpo, J. Phys. Chem. B 109 (2005) 15422.
[10] C.Y. Wang, H. Groenzin, M.J. Shultz, Langmuir 19 (2003) 7330.
[11] T. Zubkov, D. Stahl, T.L. Thompson, D. Panayotov, O. Diwald, J.T. Yates, J. Phys. Chem. B 109 (2005) 15454.
[12] A. Mills, M. Crow, J. Phys. Chem. C 111 (2007) 6009.
[13] Y. Bessekhouad, N. Chaoui, M. Trzpit, N. Ghazzal, D. Robert, J.V. Weber, J. Photochem. Photobiol. A 183 (2006) 218.
[14] A. Rampaul, I.P. Parkin, S.A. O'Neill, J. DeSouza, A. Mills, N. Elliott, Polyhedron 22 (2003) 35.
[15] Y. Bessekhouad, D. Robert, J.-V. Weber, N. Chaoui, J. Photochem. Photobiol. A 167 (2004) 49.
[16] T. Tachikawa, M. Fujitsuka, T. Majima, J. Phys. Chem. C 111 (2007) 5259.
[17] R. Bacsa, J. Kiwi, T. Ohno, P. Albers, V. Nadtochenko, J. Phys. Chem. B 109 (2005) 5994.
[18] R. Asahi, T. Morikawa, T. Ohwaki, K. Aoki, Y. Taga, Science 293 (2001) 269.
[19] K. Guan, B. Lu, Y. Yin, Surf. Coat. Technol. 173 (2003) 219.
[20] M. Houmard, G. Berthomé, J.C. Joud, M. Langlet, Surf. Sci. 605 (2011) 456.
[21] T. Shibata, H. Irie, D.A. Tryk, K. Hashimoto, J. Phys. Chem. C 113 (2009) 12811.
[22] T. Shibata, H. Irie, K. Hashimoto, J. Phys. Chem. B 107 (2003) 10696.
[23] E. Aubry, V. Demange, A. Billard, Surf. Coat. Technol. 202 (2008) 6120.
[24] W.-J. Yin, S. Chen, J.-H. Yang, X.-G. Gong, Y. Yan, S.-H. Wei, Appl. Phys. Lett. 96 (2010) 221901.
[25] V. Swamy, A.Y. Kuznetsov, L.S. Dubrovinsky, A. Kurnosov, V.B. Prakapenka, Phys. Rev. Lett. 103 (2009) 075505.
[26] N.M. Ghazzal, N. Chaoui, E. Aubry, A. Koch, D. Robert, J. Photochem. Photobiol. A 11 (2010) 215.
[27] F. Vaz, L. Rebouta, P. Goudea, J.P. Riviere, E. Schaffer, G. Kleer, M. Bodmann, Thin Solid Films 402 (2002) 195.
[28] Q.H. Fan, A. Fernandes, E. Pereira, J. Gracio, Diamond Relat. Mater. 8 (1999) 645.
[29] A.Z. Sadek, H. Zheng, M. Breedon, V. Bansal, S.K. Bhargava, K. Latham, J. Zhu, L. Yu, Z. Hu, P.G. Spizzirri, W. Wlodarski, K. Kalantar-zadeh, Langmuir 25 (2009) 9545.
[30] Y. Paz, A. Heller, J. Mater. Res. 12 (1997) 2759.
[31] H.J. Nam, T. Amemiya, M. Murabayashi, K. Itoh, J. Phys. Chem. B 108 (2004) 8254.
[32] E. Aubry, M.N. Ghazzal, V. Demange, N. Chaoui, D. Robert, A. Billard Surf. Coat. Technol. 201 (2007) 7706.
[33] W. Huang, J. Zhu, H.Z. Zeng, X.H. Wei, Y. Zhang, Y.R. Li, Appl. Phys. Lett. 89 (2006) 262506.
[34] H.S. Jung, J.-K. Lee, J. Lee, B.S. Kang, Q. Jia, M. Nastasi, J. Phys. Chem. C 112 (2008) 4205.
[35] H. Kozuka, S. Takenaka, H. Tokita, T. Hirano, Y. Higashi, T. Hamatani, J. Sol-Gel Sci. Technol. 26 (2003) 681.
[36] S.H. Wei, A. Zunger, Phys. Rev. B 60 (1999) 5404.
[37] N. Khan, J. Li, Appl. Phys. Letters 89 (2006) 151916.
[38] S. Sirohi, T.P. Sharma, Opt. Matter. 13 (1999) 267.
[39] Z. Wang, U. Helmersson, P.O. Käll, Thin Solid Films 405 (2002) 50.
[40] P. Babelon, A.S. Dequiedt, H. Mostefa-Sba, S. Bourgeois, P. Sibillot, M. Sacilotti, Thin Solid Films 322 (1998) 63.
[41] J. Yu, X. Zhao, Mater. Res. Bull. 35 (2000) 1293.
[42] T. Watanabe, S. Fukayama, M. Miyauch, A. Fujishima, K. Hashimoto, J. Sol-Gel Sci. Technol. 19 (2000) 71.
[43] A. Mills, J. Wang, J. Photochem. Photobiol. A 182 (2006) 181.
[44] P. Sawunyama, L. Jiang, A. Fujishima, K. Hashimoto, J. Phys. Chem. B 101 (1997) 11000.
[45] N. Sakai, A. Fujishima, T. Watanabe, K. Hashimoto, J. Phys. Chem. B 107 (2003) 1028.
[46] A. Fujishima, X. Zhang, D.A. Tryk, Surf. Sci. Rep. 63 (2008) 515.